STANFORD RESEARCH INSTITUTE
Menlo Park, California 94025 · U.S.A.

525407

FINAL

TECHNICAL REPORT

ARPA Order No. 2327, Amendment No. 2   Contract No. N00014-75-C-0434

Stanford Research Institute   Principal Investigator:
333 Ravenswood Avenue   E. R. Westerberg
Menlo Park, California 94025   (415) 326-6200 Ext. 4120

Effective Date of Contract: 1/24/75   Scientific Officer:
Expiration Date: 11/24/75   The Director, Naval Research
                                             Laboratory
                                             4555 Overlook Avenue, S.W.
   Washington D.C.   20375

TECHNIQUES FOR THE MICROFABRICATION OF
INTEGRATED OPTICAL WAVEGUIDE COUPLERS

Amount of Contract: $45,000

SRI Project No. 4008

Sponsored by Advanced Research Projects Agency
ARPA Order No. 2327, Amendment No. 2

The views and conclusions contained in this document are those of the
authors and should not be interpreted as necessarily representing the
official policies, either expressed or implied, of the Advanced Research
Projects Agency or the U.S. Government.

D D C

MAR 22 1977

D
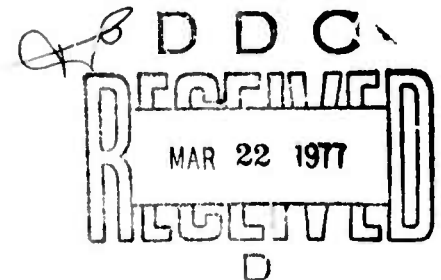
APPROVED FOR PUBLIC RELEASE
DISTRIBUTION UNLIMITED

ABSTRACT

This report covers the development of an Electron Projection
Exposure System (EPES) that uses a large-area electron beam to image
an object transmission mask with a size reduction of 20×. The demag-
nified patterns produced in an electron-sensitive resist are useful for
fabricating such devices as integrated optical couplers and switches.

ii

E. R. / Westerberg

TECHNIQUES FOR THE MICROFABRICATION OF INTEGRATED OPTICAL WAVEGUIDE COUPLERS

Final Technical Report.

Contract No. N00014-75-C-0434

SRI Project No. 4008

I INTRODUCTION

This report describes work carried on at SRI in the microfabrication of structures that are useful in the field of integrated optics (IO). IO devices are solid-state devices that can manipulate light signals by using such components as sources, detectors, modulators, and couplers, all fabricated on suitable substrates to produce systems that are much smaller than conventional optical systems. Because of the high frequency of the entrained electromagnetic waves, these components have the advantage of operating with very large bandwidths. Their small size makes IO systems much less susceptible to temperature changes, mechanical vibrations, and electromagnetic fluctuations than systems using conventional optics. Significant advantages of these systems for military application include secure communication (freedom from signal leakage), elimination of extraneous noise pickup due to grounding problems, and low susceptibility to electromagnetic interference.

The production of such structures requires advanced technology in both lithographic (pattern-production) and thin-film techniques. In particular, the requirements of the lithographic technology are stringent. Waveguides and coupling structures with guiding dimensions of only a few micrometers are required, and total device dimensions (e.g., coupler lengths in IO devices) of longer than 1 mm are necessary. Furthermore, the edge acuities of the light-guiding components must be

332 500

1

D D C

MAR 22 1977

better than 1000 Å, so that light is not scattered out of the guides to create signal-to-noise ratio and crosstalk problems. Available lithographic techniques for producing IO structures of this type fall into three categories, depending on the exposure means: light, x-ray, or electron.

Photolithography is the oldest of the techniques. Here, either the desired pattern is optically projected onto a light-sensitive resist material, or a mask is placed in direct contact with the photoresist-coated sample to produce a one-to-one copy. The photoprojection technique allows the pattern of the master transmission mask to be much larger than the final pattern, thus greatly simplifying mask production. The optical projection system then demagnifies the pattern of the transmission mask to produce a latent image in the photoresist. Because of the basic diffraction limitation imposed by the wavelength of light and the projection optics, the resolution with present-day optical projection systems is approximately 1 to 2 μm.[1]* This resolution appears to be insufficient for the production cf good 1-μm-wide optical waveguide structures.

Contact photolithography has recently made a sigificant advance with the introduction of the flexible mask.[2] The new technique employs a very thin glass mask which is placed in a vacuum frame above a photoresist-coated sample. When the frame has been evacuated, the flexible mask is forced into intimate contact with the sample surface. With this technique, resolutions of somewhat below a micron can be obtained. However, several problems arise in applying the technique to the microfabrication of integrated optical structures. Unlike the optical projection system, this technique requires the mask pattern to be the same size as the final image, and so the mask needs to be fabricated with submicron detail if the image is to contain submicron detail. Producing such a mask requires other types of lithography with higher resolution, e.g., electron beam lithography. The flexible-mask contact exposure process also suffers from a loss of edge definition because of diffraction in

---

*
References are listed at the end of the report.

the mask. Edge definition is not the same as resolution. Edge definition denotes the sharpness with which the edge of a line is reproduced, and resolution is the capability of resolving two distinct points--separated by the minimum distance. A lack of edge definition (caused by the diffraction effects in a photoresist layer of finite thickness) can lead to wavy edges on waveguides. This edge imperfection produces extra scattering and increases loss from the waveguides.

X-ray lithography uses soft x-rays to expose a suitable x-ray-sensitive resist material through a shadow mask.[3] The wavelength of the x-rays is typically 1,000 times shorter than that of visible light, and thus the resolution and the edge definition of this technique are superior to those achieved by photolithography. However, as with contact photolithography, the x-ray technique requires a mask with the same resolution as the final image.

Electron beam lithography can be classified into two categories: scanning and projection. The scanning technique uses a fine focused beam of electrons; the pattern is created in an electron-sensitive resist by appropriately deflecting this beam with a set of magnetic deflection coils. The effective wavelength of the electrons is below an angstrom, and diffraction is no problem with this technique. The resolution is generally limited by the thickness of the electron-sensitive resist, and resolutions on the order of 0.1 μm have been demonstrated. The equipment for scanning electron beam lithography is fairly complex and costly. A fabrication facility needs a scanning electron microscope (SEM) that has been modified for lithographic applications, a computer to produce the scan data, and an interfacing system to provide transfer of information between the SEM and the computer.

Two types of projection systems are used in electron lithography. In the electron image projection system (ELIPS) the pattern to be transferred is reproduced on a photocathode.[4] When this cathode is illuminated by strong ultraviolet radiation, photoelectrons are emitted in the pattern,

3

and a uniform magnetic field focuses these electrons onto the substrate surface. Large areas of exposure, high resolution, and good edge definition are possible with this technique. However, the electron optics of the process provide unity magnification, and hence pattern demagnification is not possible.

A second type of electron projection system is the analog of the optical projection system described above. It uses a transmission mask (a mask with cutout areas transparent to electrons) as an object, demagnifies this mask with an electron optical system, and projects the image onto an electron-sensitive resist surface. This system has the advantage of high resolution and good edge acuity because of the short wavelength of the electrons. It provides a projection demagnification in the range of 20 to 200X, so the transmission masks can be produced on a large scale with standard photolithographic techniques and then be reduced to the required scale with the projection system. In projection systems all portions of the image are exposed simultaneously, whereas in scanning systems the image is built up serially, one image point at a time. Consequently, the exposure times of projection systems are substantially less than the times for comparable patterns produced with scanning systems. Since an electron projection system uses a transmission mask as an object, special design attention must be given to the pattern etched into the mask, to ensure that all portions of the pattern are properly supported. For the centers of designs that would not normally be supported (e.g., the center of the letter "O"), bridge supports that are small enough so that they cannot be resolved in the image must be built into the mask.

II   THE SRI ELECTRON PROJECTION EXPOSURE SYSTEM (EPES)

The SRI EPES is an outgrowth of a one-dimensional projection system (the slit-lens exposure system) developed under ARPA Contract DAHC15-72-C-0265. The slit-lens exposure system uses a transmission mask in which a pattern of holes is transformed into a pattern of straight lines by

using a one-dimensional aperture lens (slit). Lines produced with the slit lens have high edge definition and widths as small as 0.34 μm, with interline spacings of 0.68 μm. This particular exposure system has proved useful in the fabrication of such structures as surface acoustic wave transducers, Barker-coded devices, and integrated optical waveguide masks.

The EPES uses a modified projection aperture lens to achieve two-dimensional imaging, so that a faithful image of a transmission mask can be projected onto a resist-coated substrate surface. Figure 1 shows the basic components of SRI's EPES. Electrons from a simple gun and condensing lens structure, here represented by a filament, illuminate a transmission mask. In this schematic diagram, a typical 3-dB integrated optical coupler illustrates a possible mask configuration. The transmitted electrons converge on the objective lens and an aperture lens and are focused onto the electron resist-coated substrate. Figure 2 depicts the focusing action of a simple aperture lens. The lens here is merely a round hole in a conducting plane. If the appropriate voltage is applied between this conducting lens plane and the conducting surface of the sample, the electrons will be brought to a focus at the sample surface. A higher-resolution image can be obtained by using a second aperture as a beam limiter in the field-free, object side of the lens. This aperture, with a diameter of 25 to 50% of the lens diameter, eliminates the highly aberrated electron rays that would be produced near the rim of the lens hole.

This projection aperture lens has a number of advantages. First, it is a very simple electrostatic lens. Other types of lenses require an exact registration of a number of optical elements, but this lens requires virtually no alignment to obtain high resolution. A second feature of the aperture lens lies in its self-focusing property. First-order theory shows that, if a focusing potential of 8Φ (where Φ is the energy of the electrons as they traverse the transmission mask) is applied between the lens plane and the sample, highly demagnified images will always be in focus at the substrate plane, regardless of aperture-to-substrate spacing--i.e., the EPES has a large depth of focus. This feature makes the lens system exceptionally tolerant to substrate
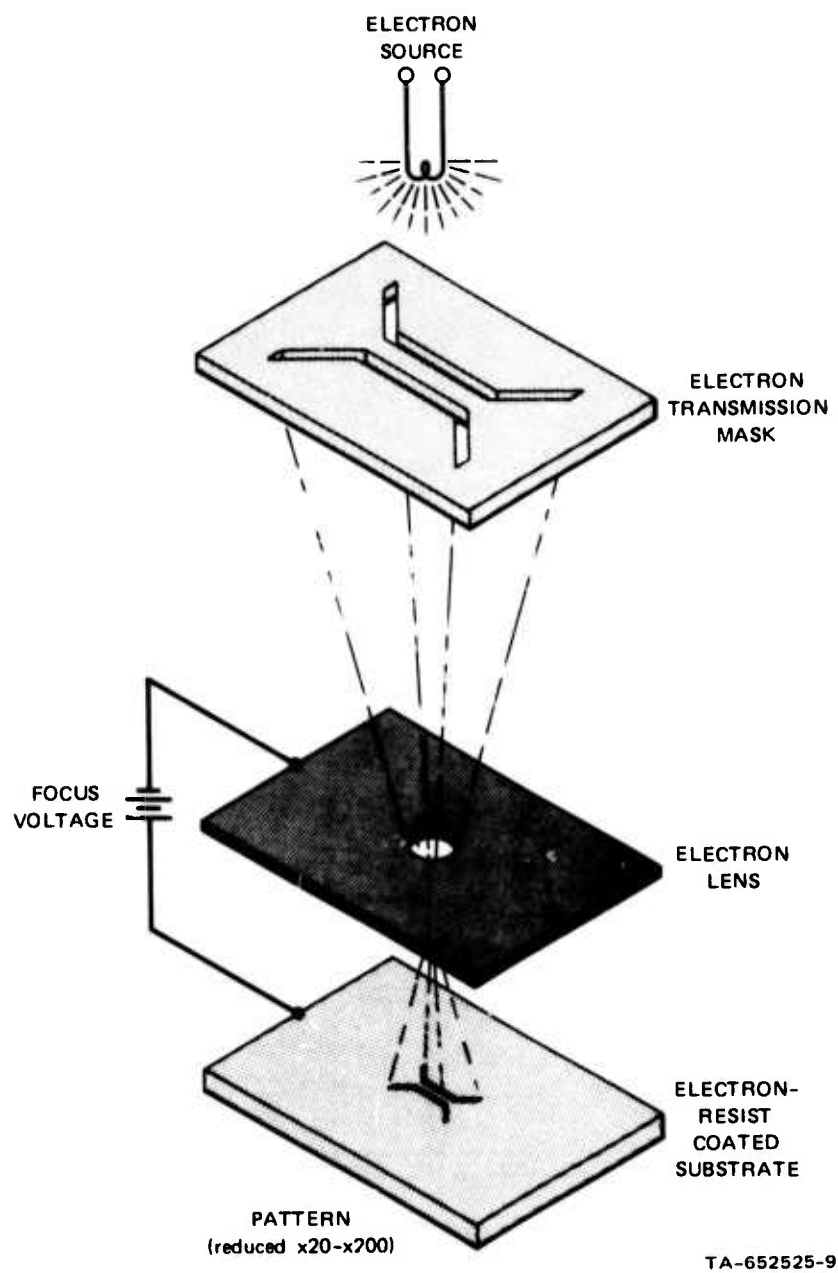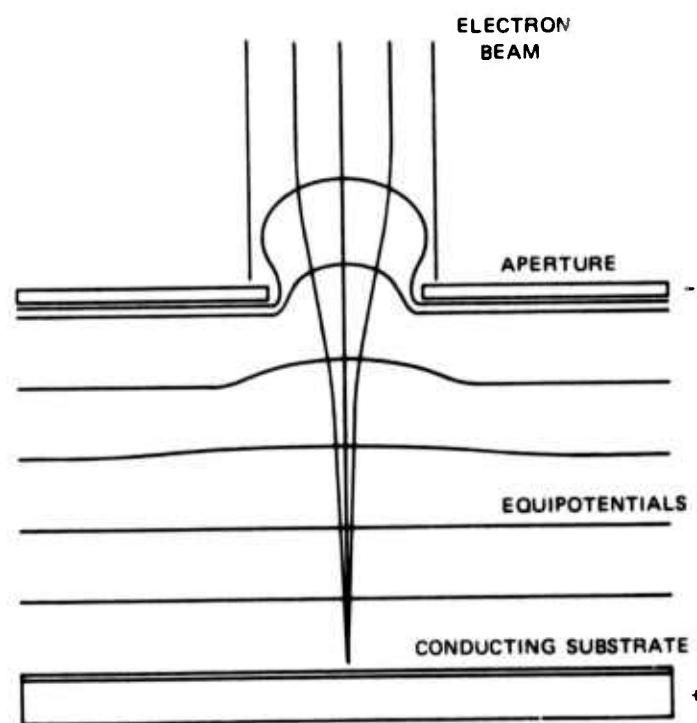
5

ELECTRON
SOURCE

ELECTRON
TRANSMISSION
MASK

FOCUS
VOLTAGE

ELECTRON
LENS

ELECTRON-
RESIST
COATED
SUBSTRATE

PATTERN
(reduced x20–x200)

TA-652525-9

FIGURE 1   ELECTRON BEAM PROJECTION LITHOGRAPHY

6

ELECTRON BEAM

APERTURE

EQUIPOTENTIALS

CONDUCTING SUBSTRATE

TA-651583-31R

FIGURE 2   APERTURE LENS ACTION

7

unevenness, which often limits the resolution of other projection and contact exposure systems. The demagnification of the EPES can be varied over a wide range by merely changing the lens-to-substrate distances. Thus, pattern production is greatly facilitated, since small magnification changes can be effected by altering the lens-substrate spacing without refocusing.

Aperture lenses possess still another interesting feature. The ultimate resolution of an electron-optical lens system is mainly determined by the spherical aberration of the system. The point-source electrons that pass near the periphery of the lens are strongly deflected to cross the axis nearer the lens than the electrons that pass through the center of the lens. This defect is called spherical aberration, and the increase in spot size is given by:

$$\delta = C_3\gamma^3 + C_5\gamma^5 + \ldots \, ,$$

where γ is the semiangle of lens illumination, and C_3 are C_5 are the third- and fifth-order spherical aberration coefficients, respectively. Ray tracing on the SRI computer has shown that the coefficients C_3 and C_5 have opposite signs for aperture lenses. Thus, when the angle γ gets large enough, the spherical aberration is partially canceled out. This enables such a lens to be used at wider apertures than is normally possible.

The SRI EPES is constructed in a modular fashion, as shown in Figure 3. The two main electron optical elements, i.e., the illumination system and the projection aperture lens, are housed in opposite ends of a fully demountable, self-aligning vacuum column and shield. Electrons from the cathode at the bottom of the column are formed into a wide beam by a grid electrode and an anode. This beam is directed through an electron lens which acts as a condensing lens. The strength of the lens is adjusted so that an image of the cathode is formed at the plane of the aperture lens. This condition ensures that as large an area as possible on the transmission mask is illuminated in the final

8

FIGURE 3   ELECTRON PROJECTION EXPOSURE SYSTEM

9

image. The transmission mask with the desired pattern is placed as close as possible to the final electrode of the condensing lens.

Two sets of orthogonal electrostatic deflectors are used to adjust the positions of the converging beam so that it is positioned on the aperture of the projection lens. The projection lens assembly consists of two components, the aperture lens proper and a beam limiting aperture plate which serves to keep the beam confined to the high resolution central region of the aperture lens. The final part of the system is the sample holder. Magnification in the system is established by the spacing between the aperture lens and the sample holder.

In more detail the EPES can be described as follows.

Gun: The gun shown in Figure 4 has a cathode of the Phillips matrix type with a diameter of 0.3 inch. The system needs a large cathode to provide a uniform illumination pattern and compensate somewhat for the spherical aberration of the condensing lens. The cathode is activated in the system by heating it to 1150°C for 5 minutes, the temperature being measured directly from the emitting surface with a radiation pyrometer. In normal operation the temperature is reduced to 1050°C. Since the entire system must be brought up to atmospheric pressure between exposures, to enable the sample to be removed, the column is backfilled with dry nitrogen before opening, to extend the life of the cathode. Typical cathodes can withstand 40 to 50 cycles to atmospheric pressure before their emission patterns grow so patchy that they cannot provide the required uniformity.

The grid electrode and anode are constructed of 316 stainless steel; each has a central 0.5-inch-diameter hole; and the interelectrode spacing is 0.5 inch. The anode is operated at ground potential, while the grid is held near the cathode potential, -500 V. The best pattern coverage seems to be obtained with the grid run slightly positive with respect to the cathode (0 to +15 V).
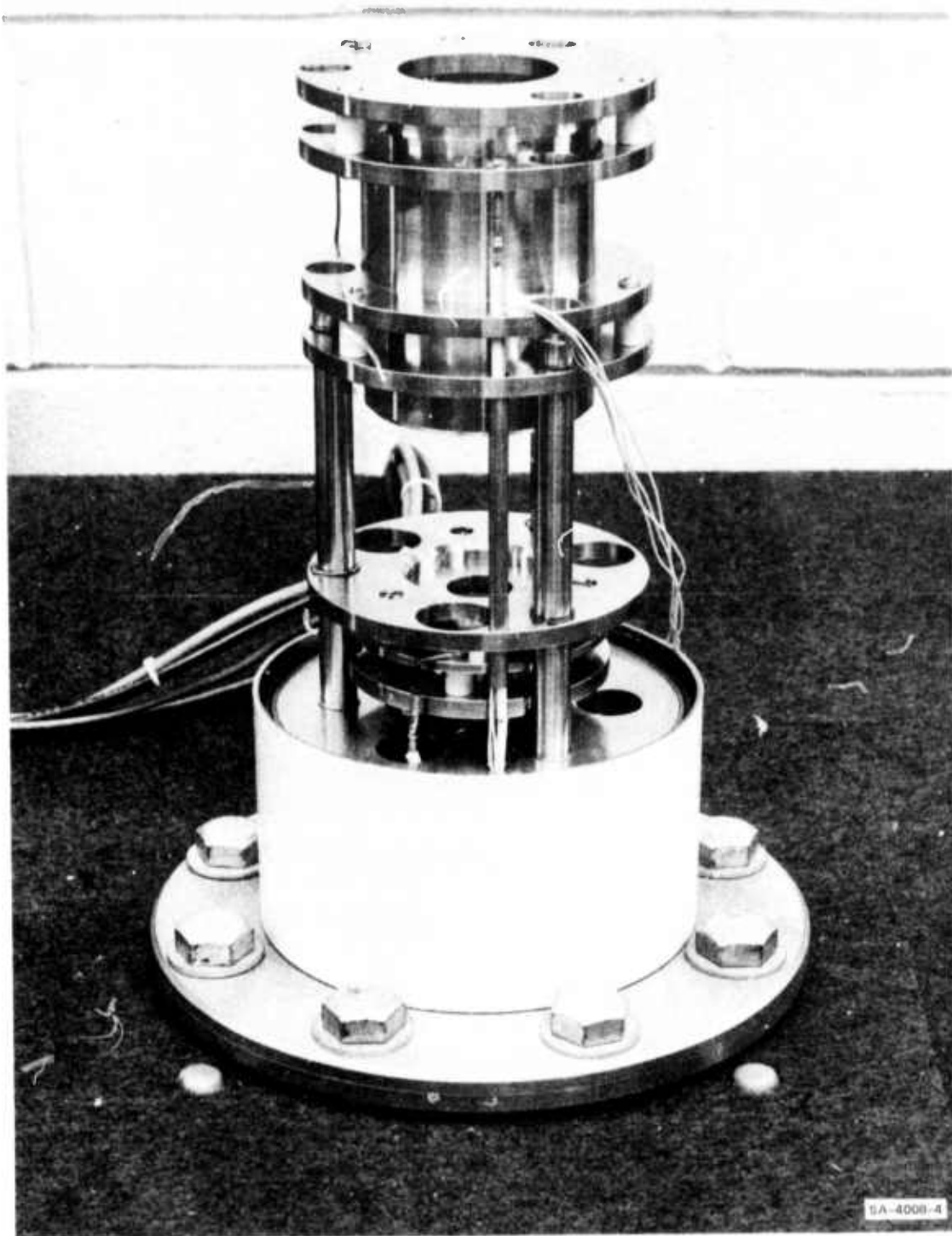
10

SA-4008-4

FIGURE 4   ELECTRON GUN

11

Condenser Lens: The top of the gun shown in Figure 4 is the condensing lens structure. The structure is built in an erector-set fashion on a set of three supporting rods. This configuration makes it easy to modify the illumination system. Several lens configurations were assembled and tested. Performance depends mainly on the spherical aberration of the lens, which shows up as an unevenly illuminated image on the sample surface. Since the transmission mask is positioned very close to the condenser lens, portions of the pattern near the periphery are illuminated by electrons that are considerably off axis in the condenser lens. The spherical aberration causes these marginal electron rays to be focused closer to the lens than the paraxial rays, i.e., those through the lens center. Thus, if the paraxial rays are focused on the projection lens, the overfocus of the marginal rays prevents them from contributing to the image, and the spherical aberration establishes the maximum pattern diameter that can be produced.

The best lens configuration that we have determined for the condenser is the einzel lens, a three-electrode lens in which the outer two electrodes are run at ground potential and the inner electrode near cathode potential, i.e., typically 50 to 100 V positive with respect to the cathode. The lens plates for this configuration have a relatively large bore (2.00-inch diameter), and the interelectrode spacing is 1.00 inch. An aperture in front of the lens limits the entering rays to a bundle of about 1-inch diameter. The focal length of the lens is approximately 7 inches. Third-order spherical aberration limits the effective area of illumination to 0.4 inch at the transmission mask plane.

Substantial improvements in illumination areas are very difficult to realize by further improvements in condenser lens design or spherical aberration reductions. Since the aberration diameter at the beam-limiting aperture plane is proportional to $C_s d^3$, where C_s is the spherical aberration coefficient and d is the beam diameter at the mask, a decrease in C_s of almost 16 times must be achieved to effect an increase of d

12

from 0.4 inch to 1.0 inch. This problem was examined theoretically, and no lens configuration was found that would give such a large spherical aberration reduction.

We used another approach to increase the effective area of illumination. If an alternating potential is applied to the center electrode of the condensing lens, the focus of the lens is continuously altered so that some of the marginal rays of the condenser lens can be brought to focus through the projection lens. We built a focus control system for the condenser that allows various ac waveforms to be superimposed on the dc focus potential. Sine, triangle, square, and ramp waveforms were tested for the best illumination characteristics. Sine waves proved to be the most useful and we were able to extend the illumination area diameter from 0.4 inch to 0.55 inch by applying a sine wave of 15 V_{rms} to the center electrode (dc potential $\sim$ -450 V). The method is not perfect because the marginal rays pass through the beam-limiting aperture only periodically, whereas the paraxial rays are focused virtually continuously, resulting in a pattern with a bright central region.

Transmission Mask Positioner: With electron projection, each transmission mask pattern is reduced to cover an area with side lengths of about 0.65 mm, but to fashion entire IO devices it is necessary to cover a length of 2 mm or more. Since this cannot be accomplished in a single exposure with our system, we built a transmission mask positioner into the EPES. This positioner enables us to change patterns without breaking vacuum; when it is used in conjunction with an accurately positionable sample stage, we can register a number of patterns on the substrate and thus form an extended pattern by sequential exposure.

The mask positioner is shown in Figure 5. It has provisions for eight independently alignable masks. Each mask is 0.75 inch square. The positioner was built to fit our 6-inch-diameter column as a modular unit. However, to accommodate eight masks, the diameter of the unit was increased to 14 inches. All the masks are mounted on a large rotary stage that can be turned from outside the exposure system through a
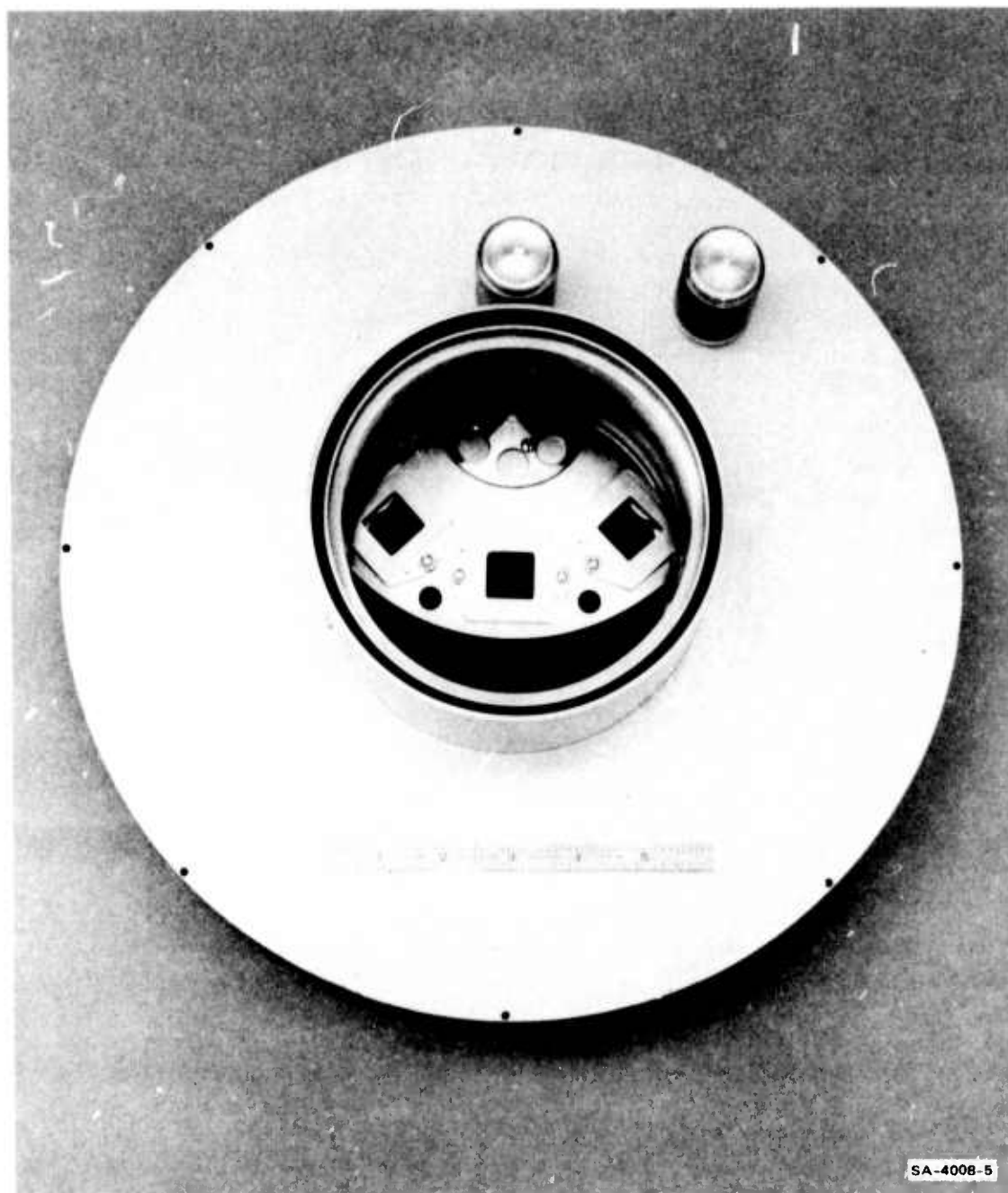
13

SA-4008-5

FIGURE 5   TRANSMISSION MASK POSITIONER

vacuum seal, and the alignment of the mask pattern is ensured by use of a hardened tapered pin as an alignment dowell. This pin was hand-lapped to give positional repeatability of better than 2 μm. The entire rotary positioner can be easily removed from the projection system and placed under a toolmaker's microscope where each mask can be aligned independently to an accuracy of 0.0001 inch. After electron optical 20X reduction, the error is of the order of 1000 Å and should be tolerable for IO devices.

Deflectors: As can be seen in Figure 6 the beam-positioning deflectors are simple electrostatic plates placed immediately after the mask holder. Because of the small deflection angle, generally less than 10 mrad, there is no need to optimize their design for low aberration. Deflection voltages are applied differentially, and for alignment dc voltages of about +20 V are required for the 500-eV beam.

Projection Lens: The heart of the EPES is the aperture lens (Figure 7) that serves to demagnify the pattern on the transmission mask. It is a simply constructed lens consisting of two plates, a beam-limiting aperture plate, and a plate with a somewhat larger diameter hole that functions as the lens proper.

We made theoretical study of aperture lenses to determine the resolution capabilities of various lens designs. Figure 8 summarizes the results of this work. This figure depicts the normalized radius of the circle of least confusion as a function of the normalized aperture radius; i.e., it shows how resolution is limited by the third-order spherical aberration as the aperture of the lens is increased. Here, δ_{CLC} is the radius of the disc of least confusion; R is the radius of the projection lens; a is the radius of the beam-limiting aperture; Z_i is the lens-to-sample spacing; and C_3 is the third-order spherical aberration coefficient. It is interesting to note that the curves tend to follow the shapes predicted for third-order spherical aberration up to a definite point, after which higher orders (fifth, predominantly) take over, and the curves actually have less total aberration than
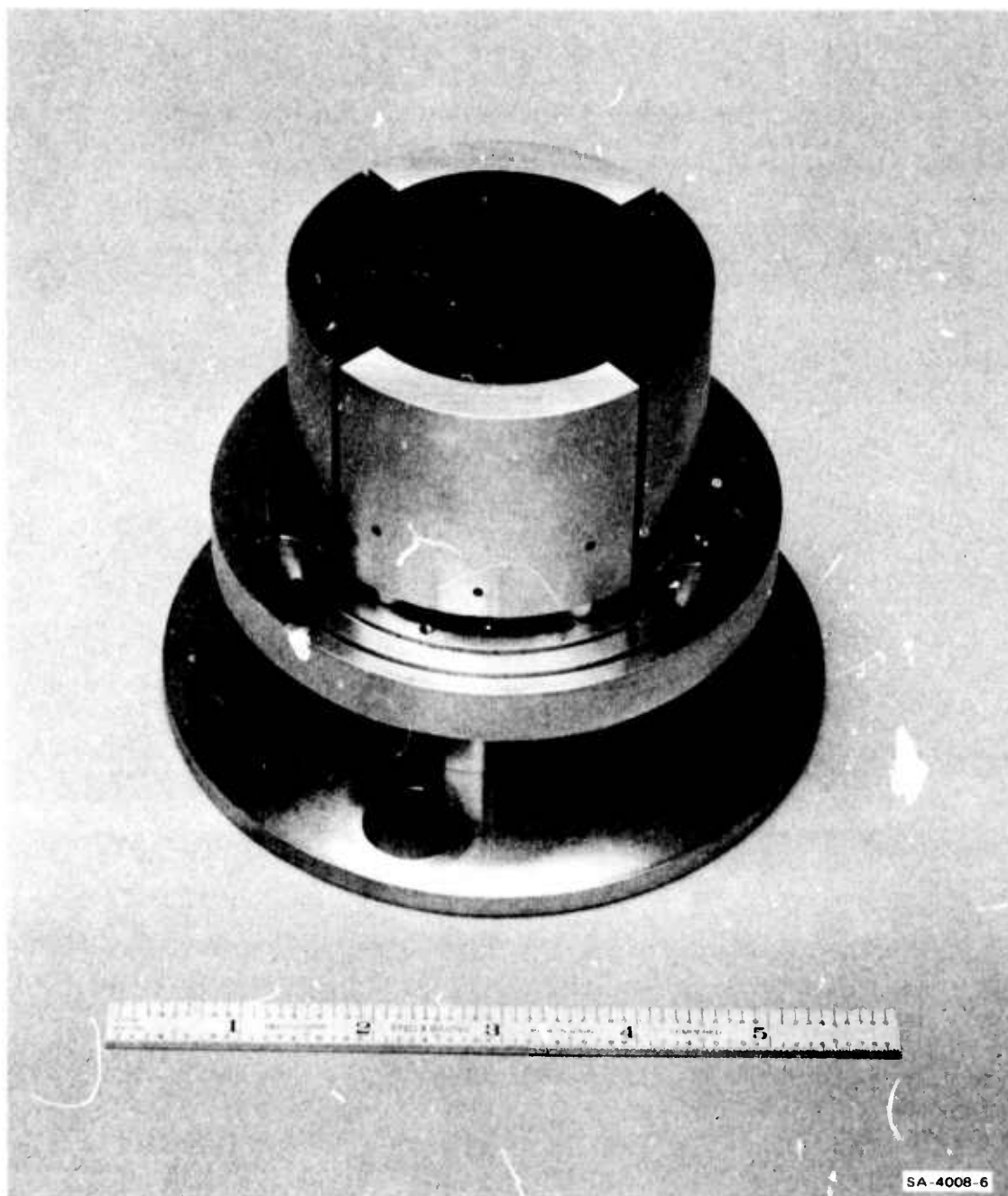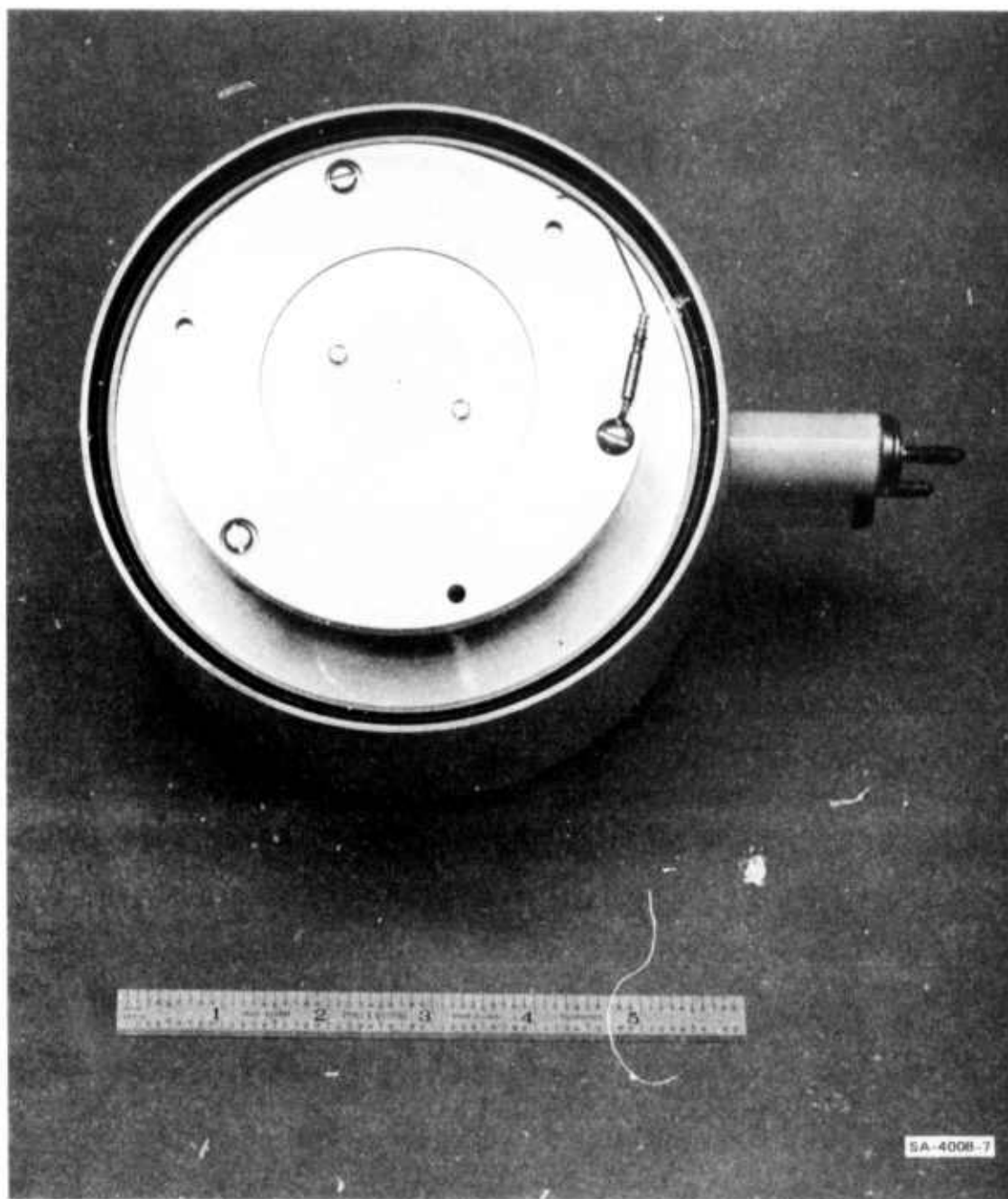
15

FIGURE 6   DEFLECTORS
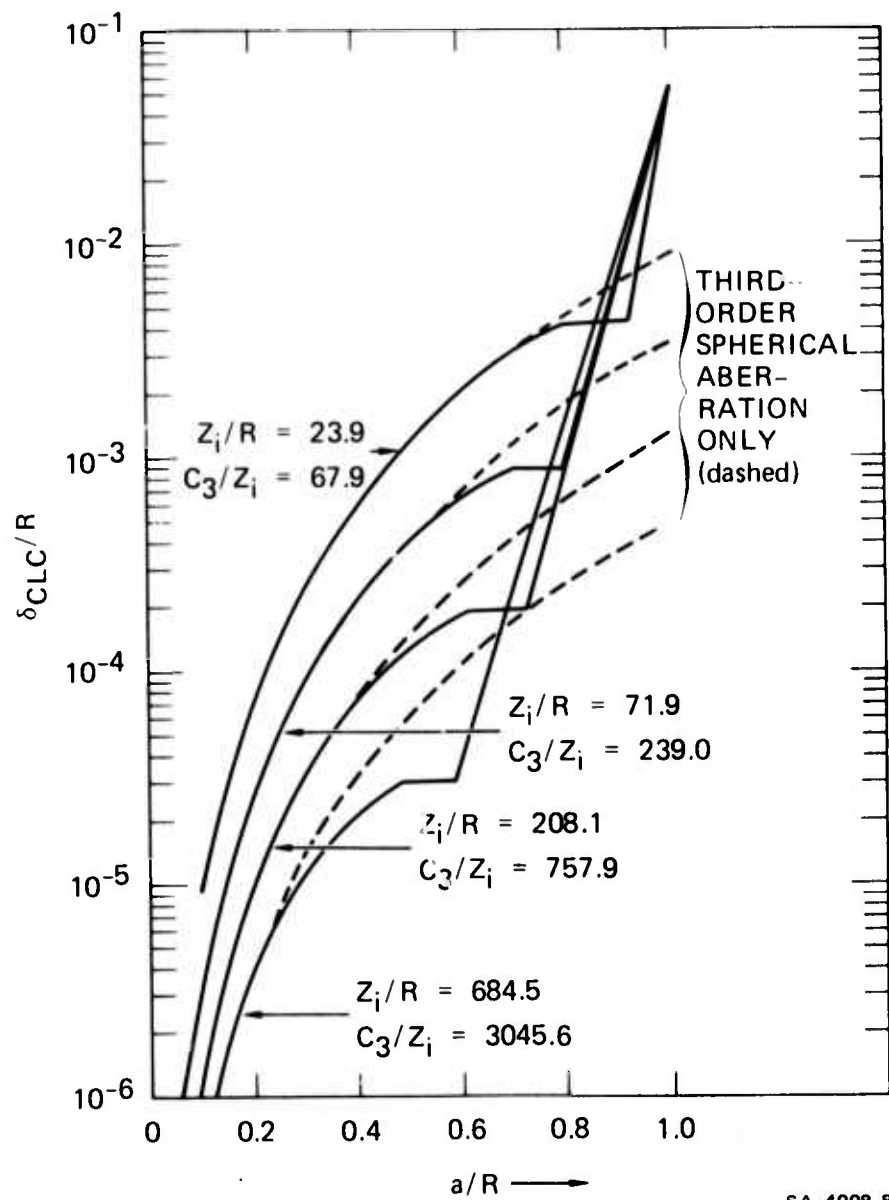
16

FIGURE 7 PROJECTION LENS AND HOLDER

17

FIGURE 8   APERTURE LENS SPHERICAL ABERRATION

SA-4008-8

18

third-order theory alone would predict. In fact, each curve reaches
a plateau during which there is no increase in the circle of least con-
fusion until suddenly, at nearly full aperture, the curves start to in-
crease in an exponential manner. The fact that the aperture lens possesses
a negative fifth-order spherical aberration coefficient should make it
a very useful imaging lens since normally the higher-order coefficients
add more aberration rather than partially correct lower orders.

Our first projection lens consisted of a beam-limiting aperture
plate 0.003-inch thick with a 0.005-inch-diameter hole and a lens plate
0.005 inch thick with a 0.010-inch-diameter hole. Separation was 0.030
inch, and the holes were aligned on a mutual axis by adjustment under
a 100X toolmaker's microscope. The lens-sample spacing was 0.360 inch.
The Z_i/R ratio was ~ 72.0; i.e., the second curve from the top of Figure 8.
At $a/R = 0.5$, $\delta_{CLC}/R \simeq 4 \times 10^{-4}$, or the resolution should be about 500 Å
$(2\ \delta_{CLC})$.

In an effort to partially overcome the effects of the spherical
aberration of the condenser lens, we experimented with several other
lens combinations. With a larger beam-limiting aperture, it would be
expected that more of the spherically aberrated marginal rays would be
imaged on the sample, and hence the effective area of illumination would
be increased. We used a larger-diameter projection lens (0.020-inch
diameter) and beam-limiting apertures of 0.010 inch diameter and 0.016
inch diameter. Theoretical resolutions with a $Z_i = 0.500$ inch are 3000 Å
for the 0.010-inch diameter aperture and 5000 Å for the 0.016-inch
diameter aperture. Resolution tests made on PMM resist showed a reso-
lution of about 5000 Å for both lenses. The measurements show reason-
able agreement with the theory. The first lens may not have performed
as well as predicted because of several factors. Astigmatism is not
taken into account in the calculations, and a small misalignment in the
lens axes might have increased its contribution. The resist had a thick-
ness of about 2000 Å; within this thickness there will be some reso-
lution degradation because of extra scatter. A significant increase
in the area of uniform illumination occurred when the two lenses were

19

used. In the case of the 0.010-inch- diameter aperture this area increased from 0.55-inch diameter (with ac on the central condenser lens electrode) to 0.60 inch, and with the 0.016 inch-diameter aperture the area diameter increased to 0.75 inch.

Sample Holder: The sample holder was designed for use in conjunction with the rotary mask holder to produce extended coupler patterns. By rotating a new mask into the electron beam and precisely moving the sample in one direction, a series of pattern images can be placed on the sample, each aligned with the previous pattern to make an entire coupler. The stage for the sample holder is shown in Figure 9. Basically, it is a modified translation stage manufactured by Aerotech, Inc. (Allison Park, PA). It was reworked and lubricated to function within a vacuum system at pressures as low as 5×10^{-7} torr. It uses a crossed-roller principle for lateral stability and has a precise linear motion virtually free of backlash and extraneous sideways motion. Positional accuracies of 1 millionth of an inch (250 Å) are claimed to be possible with this stage, and it will traverse distances of up to 2 inches. A laser-controlled interferometric system is used to measure the position of the stage. This system is manufactured by Holograph, Inc., (San Carlos, CA). The stage (within the vacuum system) is connected directly to the interferometer via a rod that passes through an o-ring seal in the vacuum wall. The interferometric system incorporates a precision glass scale ruled with a pattern of interfering light fringes. The position of this glass scale is monitored by counting interference fringes as the scale is moved. Air bearings are used to reduce the sliding friction. The accuracy of the Holograph stage is about an eighth of a fringe of red light (better than 1000 Å).

In addition to the sample holder, the stage incorporates a Faraday cup for measuring the total beam current and a transparent phosphor screen that can be viewed with a low-power microscope attached to the top of the EPES. The microscope allows the general detail of the pattern to be viewed for the initial setup. Phosphor resolution is sufficient
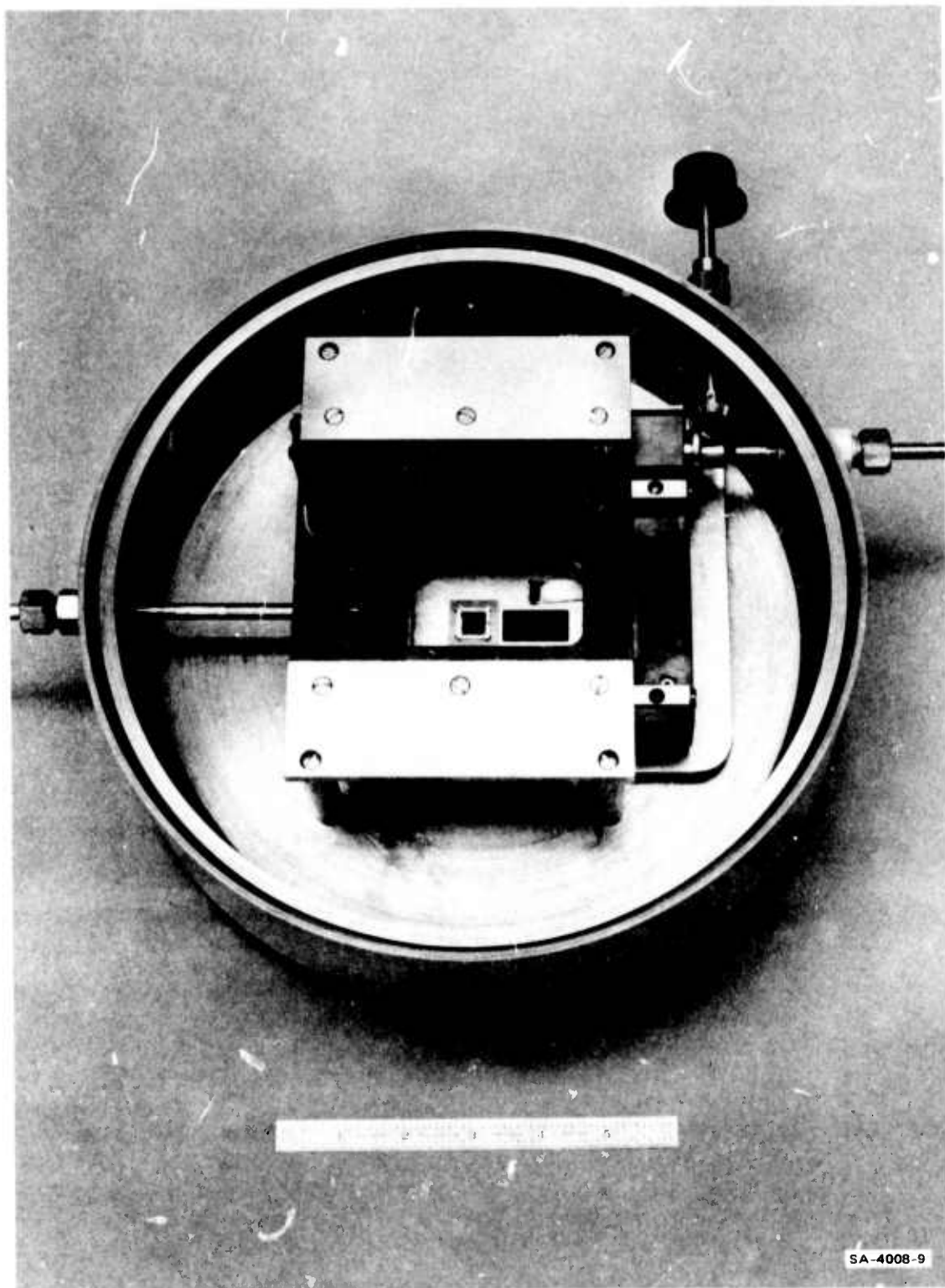
20

SA-4008-9

FIGURE 9   SAMPLE HOLDER

21

to enable the operator to produce the most uniformly illuminated image, but it is not good enough to allow the proper focus to be determined. Focus can be determined only by trial-and-error exposure of a number of different samples.

The sample holder is mounted directly to the stage, but it is insulated from it for a potential difference of 7000 V. The exposure time is controlled by using the sample potential as an electronic shutter. The beam is cut off from the sample when its voltage is made about 15 V more negative than the cathode voltage (-500 V), and for exposure the sample voltage is abruptly changed to about -8.3 times the cathode voltage ($\sim$ +4150 V). This method of shuttering has the advantage that between exposures the electron beam is shut off only in the very short region between the projection lens and the sample ($\sim$ 0.5 inch) and remains stable in the rest of the column. This stability is important, because the energy of the beam before the final lens is only 500 eV and is easily deflected by charge that can build up on interior surfaces. Exposure times are typically of the order of 10 seconds but can be as short as 1 second.

Tests were made on the resolution of the EPES by using a fine mesh screen supported over a 0.055-inch-diameter hole as a transmission mask. The intermesh spacing of the screen (50 .8 μm) was demagnified by 19.2X and projected onto a silicon wafer coated with PMMA. A typical pattern obtained after development is shown in Figure 10 where the distance between adjacent exposures is 2.6 μm. The resolution demonstrated by this method is about 0.5 μm and should be adequate for IO devices.

III   FABRICATION OF ELECTRON TRANSMISSION MASKS

Fabrication of suitable electron transmission masks to form the uniform incident electron beam into the desired spatial pattern are essential for the successful production of the desired IO coupler pattern. Several conditions must be met for useful electron projection masks. Since the definition of the final coupler edge should be held to an

22

acuity of 500 Å or better, a close tolerance ($\sim$ 1µm at 20 X reduction) is placed on the edge roughness permitted in the object mask pattern. Furthermore, the transmission masks must be made with effective support for the fine structure in the pattern. The pattern must withstand normal handling without developing defects; it must be sturdy enough that the pattern edges do not vibrate during exposure and destroy the edge resolution, and it must withstand the heating effect of the impinging electron beam.

We tried various methods of producing the high-resolution, structurally stable electron transmission mask needed for the EPES. The basis of these methods is the use of standard contact photolithography. Because of the electron projection reduction of 20X, the use of photolithography is adequate to produce masks with the needed definition. The selective etching properties of silicon and metal films are used in the microfabrication process.

All the methods of making masks entail the use of silicon as a backing layer for a thin film of metallic gold in which the high-resolution pattern is etched. The silicon backing material is etched away preferentially to a slightly larger size than the pattern in the gold. This technique leaves the gold overhanging the edge of the silicon slightly to provide a high-definition pattern.

Basically, three techniques for the production of transmission masks were developed during this contract. The first technique consists of etching the silicon support with a nonselective plasma etch with SF_6 gas. A num' r of masks were made with the technique, but it was found very difficult to control the silicon etch rate uniformly over the sample, and frequently either the silicon support was removed completely or thin remnants of incompletely etched silicon remained behind in the transmission area. To increase the yield, a second technique using a selective etch process was tried. This method uses the orientation-dependent characteristics of silicon to certain aqueous etchs, in particular to a 44% KOH solution heated to 85°C.[5] The selective etch enhances the depth to which the pattern can be etched into the top silicon surfaces
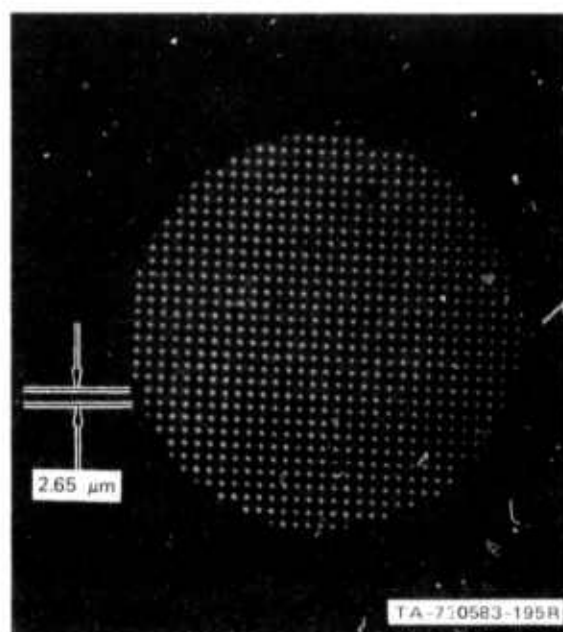
FIGURE 10   RESOLUTION OF A PROJECTION LENS

without grossly undercutting the gold film as a nonselective etch would. The deeper pattern makes it easier to etch the wafer from the back without losing the silicon support. This technique was not entirely successful, because certain portions of the coupler pattern did not align exactly with the slow etching (111) planes of the silicon, and ragged edges resulted where the patterns tended to curve.

The third technique proved to be very successful, and substantially increased the ease of mask fabrication. This method relies on the fact that highly-doped silicon etches at a much slower rate than undoped silicon with certain etches [5]. Thus, if the silicon immediately adjacent to the gold layer is heavily doped, e.g.,with boron, then, when the etch is applied to remove the silicon in the pattern areas, the etch will slow down when it comes to within about 1 μm of the gold layer, because of the indiffused boron. This property makes it possible to obtain a final uniform thickness of silicon under the gold film to add to its mechanical support. Initial masks were produced with an aqueous silicon etch composed of ethylene diamine-pyrocatechol and water heated to 115°C in a reflex condenser. The fragility of such thinly etched masks made them difficult to handle in the hot aqueous etchant, and the aqueous technique was replaced by a gaseous etching technique using SF_6. This change of etchants increased the mask yield substantially, and subsequently all masks have been fabricated by SF_6 etch methods exclusively.

In detail the transmission masks are produced with the following sequence of steps.

1.   A 2-inch diameter wafer of [100] Si, 0.013 inch thick and polished on one side is washed in methanol, followed by ultrasonic agitation cleaning in isopropyl alcohol, rinsed in a flowing isopropyl alcohol solution and blown dry with a clean stream of warm, dry nitrogen.

2.   A thin film of dopant solution is spun onto the clean wafer at a speed of 4500 rpm. The dopant we used is Emulsitone's Type-B Borofilm (Emulsitone Co pany, 19 Leslie Court, Whippany, NJ). This procedure produces

25

dopant concentrations in excess of 2×10^{19} cm^{-3}.

3. The wafer is heated to 1150°C in a tube furnace for 1 hour in an argon atmosphere.

4. The diffusion of boron into the top surface of the wafer is completed with a 25.4-hour heating period at 1200°C. The final depth of diffusion is about 12 μm.

5. As a by-product of the last step, a heavy oxide film is formed on the wafer surface. This layer is removed in a solution of HF and H_2O (1:1) at room temperature.

6. The wafer is now diced into squares .75 inch on a side.

7. The dice are ultrasonically cleaned in isopropyl alcohol to remove the Si fragments created by the dicing operation and are then blown dry with warm nitrogen.

8. The surfaces are sputter cleaned in an RF sputter unit; a deposit of SiO_2 is then sputtered on, to a thickness of about 1500 Å.

9. A thin layer of chromium (1000 Å), followed by 1.2 μm of gold, is next sputter deposited (approximately a 1-hour deposition at 300 V).

10. Shipley positive photoresist AZ-111 is spun onto the gold to a thickness of 6000 Å (3500 rpm spinner speed) and then baked at 70°C for 20 minutes.

11. The pattern is exposed in a mask aligner with an ultraviolet lamp. A typical exposure time is about 4 seconds.

12. Development is carried out in a 1:4 mixture of Shipley developer and H_2O for 30 seconds. The surface is dried in a nitrogen stream.

13. Post-baking is done in two steps: a drying operation at 70°C for 2 hours and a resist-hardening step at 170°C for 20 minutes.

26

14. The gold film unprotected by the resist is sputtered away. This process takes about 2 hours at 1000 W RF. During this etch some of the silicon dioxide is also removed.

15. The remaining oxide is etched with a standard buffered oxide etchant (BOE).

16. The boron-doped silicon in the pattern is then removed to a depth of 10 to 15 μm, with a mixture of HF and HNO_3 (3:7). An etching time of 20 to 30 seconds is generally sufficient.

17. To protect the pattern in subsequent processing, the etched channel is filled with a mixture of AZ-111 and monochlorobenzene (3:1). Care must be used in applying this mixture so that no air bubbles become trapped in the pattern.

18. The AZ-111 filler is dried at 70°C for several hours.

19. The silicon die is now inverted, and the area surrounding the pattern is masked with an alumina mask. Metal masks seem to affect the etch rate, and the result is a slower and less uniform etching. Areas not easily protected by the alumina mask can be coated with a layer of AZ-111, but this layer will probably need to be renewed several times during the plasma etching process. The plasma etching uses SF_6 gas at a pressure of 250 microns. The gaseous discharge is sustained with a voltage of 600 V rms and a power of 75 W. The etch rate decreases markedly when the undiffused boron layer is reached, and the etching can be observed directly to determine when the pattern is complete.

20. The AZ-111 filler is removed in acetone, followed by a flush with isopropyl alcohol and hot dry nitrogen.

27

21. As a final step, gold is deposited on the back side of the silicon die. This operation has two effects. It coats the back of the exposed SiO_2 with a conductive layer to reduce charging during use in the EPES. Furthermore, with no coating the tension of the gold on the front side of the mask tends to curl the thin supporting membrane; by coating gold on the reverse the tension is compensated and the mask curl is reduced.

IV IO COUPLER DESIGN

For the project we designed and fabricated two optical masks for transmission mask production. Figure 11 shows the two mask patterns used for initial mask fabrication tests. These two masks include one that produces a region of high coupling and one that produces a low coupling region. The masks are designed so that their images can be juxtapositioned with the EPES rotary mask holder and sample stage.

The high coupling region is sandwiched between two low coupling regions that serve as inputs and outputs. Approximate theories[6,7] were used to establish the critical dimensions of the simple mode waveguides and coupler region.

When the patterns are reduced twenty times by electron projection, the 70 μm wide line should produce a single-mode guide in the diffused lithium niobate ($\Delta n \sim 0.01$). The line separation (in the high coupling region) was calculated to give about 3-dB coupling over the close proximity region. The smooth areas of the separation region were designed to yield low loss[8] (< 1 dB) and are tapered at 10 degrees to the axis. In the overlap region, where the two patterns are to be joined, the line width narrows by 20 %. This arrangement compensates for any line broadening effect of having two electron-beam exposures in this region. The low coupling region was designed to provide:
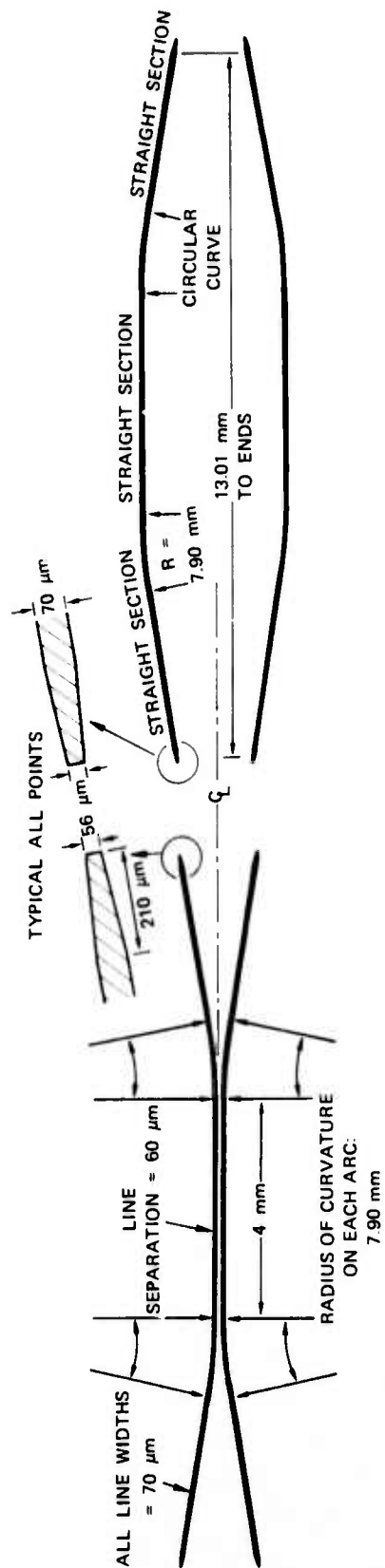
(a) HIGH COUPLING REGION

(b) LOW COUPLING REGION

(c) COMPOSITE

SA-4008-2R

FIGURE 11 OBJECT MASK PATTERNS FOR IO COUPLER

29

- Nearly zero power exchange between guides

- A region where phase-shift electrodes can
  be formed if a switch is to be made.

The optical masks, obtained from Bell Industries (Photomask Division, 1165 Fairoaks Ave., Sunnyvale, CA.), were of reasonably good quality. However, they suffered small systematic faults that may be attributed to the manner in which the computer-generated patterns were composed. Specifically, the discrete digital motion of the light exposure apparatus produces small steps along regions that should have continuous arcs. This may be a problem for the highest-quality IO patterns and would be difficult to eliminate because the digital stepping is inherent in the photomask production technique.

Several transmission masks were fabricated in gold on silicon by using the process discussed in the last section. Both sections of the IO patterns were fabricated. Figure 12 shows the etching of the coupler legs on a mask of the high coupling region. Good definition of the waveguide regions was obtained with the mask fabrication procedure. In general, the edge smoothness of the transission masks was less than 1 μm, giving a theoretical edge roughness in the inal pattern (after 20X reduction) of less than 500Å.

The low coupling pattern was the easier to fabricate because there was ample material for support between the long cut-out waveguide sections. However, the high coupling region presented some extra fabrication problems, because the long support distance (4 mm) between the two waveguides is only 60 μm wide. A mask was successfully fabricated with the technique, but, in general, masks of this design are too fragile to be practical. To overcome the breakage problem, The mask was redesigned to have only one leg of the coupler, (i.e., imagine the pattern in Figure 11 bisected between the two waveguides). This design completely eliminates the fragility problem because all portions of the mask are strongly supported. Two identical waveguides of this type are fabricated
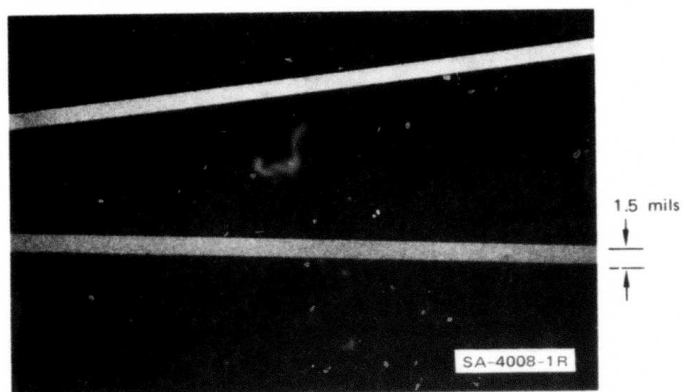
30

1.5 mils

SA-4008-1R

FIGURE 12   TRANSMISSION MICROGRAPH OF OBJECT MASK PATTERN

31

and then positioned in the rotary mask holder so that by exposing each mask in sequence, the entire high coupling region is imaged onto the sample. Dividing the high coupling region between two masks has the added advantage that the coupling distance between the two waveguides can be adjusted when the masks are lined up under the toolmaker's microscope. Thus it is possible to change the coupling distance without having to produce a new photomask and then fabricate a different transmission mask. Several of these split high coupling region masks were produced for use in the EPES.

## V   FABRICATION OF DIFFUSED WAVEGUIDES IN $LiNbO_3$

The method we used to form optical waveguides is a diffusion technique. Figure 13 illustrates the method in contrast with an etching process that leaves the guiding material standing proud on the substrate as an alternative to indiffusion.

In our work, transition metals, specifically titanium, were diffused into the $LiNbO_3$ crystal to form a higher index region at the surface. Three factors determine the waveguide properties: the Ti thickness, the diffusion temperature, and the diffusion time. The details of the process are as follows.

1.   Clean the polished Y-cut $LiNbO_3$ crystals (obtained from Crystal Technology). Cleaning is best done by starting with a gentle ultrasonic agitation in a methanol solution, followed with an isopropyl alcohol rinse, and drying with a flow of warm nitrogen. A light sputter etch in an oxygen plasma serves to eliminate any organic residuals on the surface.

2.   Coat the clean $LiNbO_3$ with a thin film $\sim$ 1500 Å thick of electron-sensitive resist material, polymethyl-methacrylate (PMM). This operation is performed on a resist spinner at about 4500 rpm.

METHOD A — DEPOSITION

STEP 1 PRODUCE HIGH-RESOLUTION PATTERN ON SUBSTRATE BY ELECTRON-BEAM EXPOSURE OR OPTICAL EXPOSURE OF RESIST.
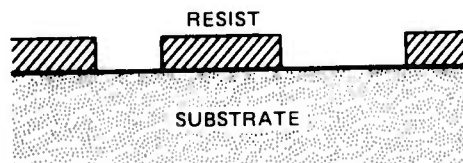
RESIST

SUBSTRATE

*STEP 2* DEPOSIT INDIFFUSION SOURCE METAL TO DESIRED THICKNESS AND LIFT OFF UNWANTED RESIST.

TITANIUM

t_1 t_2
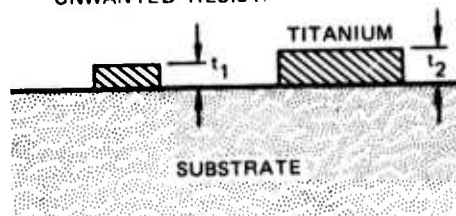
SUBSTRATE

STEP 3 HEAT SUBSTRATE TO CAUSE METAL IONS TO INDIFFUSE. DIFFERENT METAL THICKNESSES CAUSE DIFFERENT INDICES.

t_1 t_2

SUBSTRATE

n_1 n_2
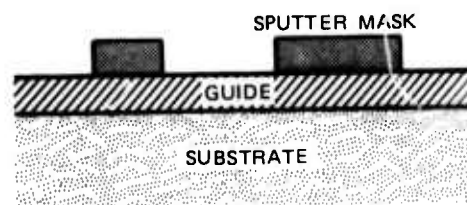
INDIFFUSED REGIONS
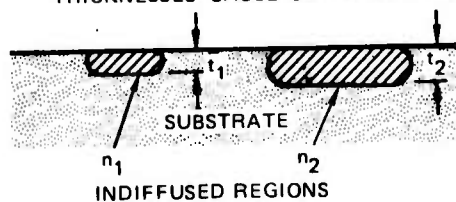
METHOD B — ETCH

STEP 1 COVER ENTIRE SUBSTRATE WITH METAL AND INDIFFUSE A UNIFORM GUIDE LAYER.

GUIDE

SUBSTRATE
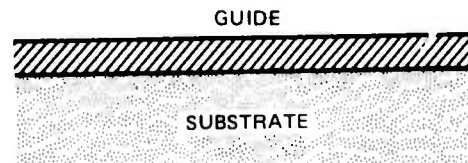
STEP 2 PRODUCE HIGH-RESOLUTION PATTERNS ON THE GUIDE, USING A SPUTTER-RESISTANT MATERIAL AS A MASK.

SPUTTER MASK

GUIDE

SUBSTRATE

STEP 3 SPUTTER ETCH PATTERN INTO THE GUIDE. SPUTTER MASKING MATERIAL CAN BE SELECTIVELY REMOVED.

GUIDES

SUBSTRATE
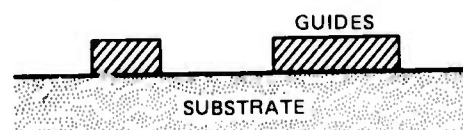
SA- SA-652525-8R

FIGURE 13   TECHNIQUES FOR FORMING OPTICAL COMPONENTS IN INDIFFUSED WAVEGUIDES

33

3. Apply a drop of antistatic solution [available from Ernest Fullam, Inc. (Schenectady, N.Y.)] and spread uniformly by spinning at 4000 rpm. This antistatic material lowers the surface resistivity of the PMMA and allows trapped charge to dissipate, so that the pattern does not become distorted by electrostatic forces during electron beam exposure.

4. Secure the sample to a holder with a conducting silver cement, making sure that the antistatic layer is connected to the holder. Place the holder in the EPES and expose for the required time (generally 10 to 30 seconds).

5. After extraction from the EPES, remove the silver cement and develop the latent image in isopropyl alcohol for 1 minute.

6. After visual inspection of the pattern, deposit $\sim$ 500 Å thickness of Ti metal onto the sample surface with an electron-beam evaporation system. Thickness is controlled with a crystal monitor.

7. To remove the unwanted portions of the Ti film, gently ultrasonic the sample in an acetone bath. The undercut of the PMMA resist due to backscattered electrons delineates the Ti pattern on the $LiNbO_3$ surface and physically separates it from the Ti on the surface of the PMMA. The latter is removed during the ultrasonically aided dissolution of the resist film.

8. Clean the sample surface in isopropyl alcohol, and blow dry with N_2.

9. Place the sample in a diffusion furnace. Flow on inert gas (N_2 or A) over the sample, and slowly (over the period of several hours) bring the temperature up to 1050°C. Slow heating is a necessity because of the

danger of thermal shock and subsequent cracking of the $LiNbO_3$. The crystals seem to be highly stressed and are very temperature gradient sensitive. Do not exceed 1125°C, the Curie temperature of $LiNbO_3$, or the sample must be repoled. One must be sure that both the tube and the carrier are free of contamination. A platinum boat seems to be a good sample carrier, because it is inert and it allows good heat exchange with minimum temperature gradients.

10. Diffuse for the necessary length of time. A times of 27 hours produces four propagation modes, and single-mode guides can be formed in about 10 hours.

11. Allow the furnace to cool slowly in an oxygen-rich atmosphere, to replace oxygen lost from the lattice during diffusion. Cooling should be done over a period of at least 5 hours, with the slowest rates of cooling taking place initially when the sample temperature is the highest. The crystal should be removed only when it reaches room temperature, and it will be clean with a very slight grey tint.

Indiffused planar guides (without electron-beam pattern delineation) were produced and tested. Both photodiode probe and photographic measurements were made of the attenuation of optical waves (λ = 6328 µm) in several $LiNbO_3$ indiffused guides, and we found the net optical loss to be less than 1 dB/cm. Thus high-quality low-loss layers can be routinely produced by this technique.

35

REFERENCES

1. L.I. Maissel, and R. Glang, eds., <u>Handbook of Thin Film Technology</u> pp. 7-18 (McGraw Hill, New York, New York, 1970).

2. H.I. Smith, F.J. Bachner, and N. Efremow, "A High Yield Photo-lithographic Technique for Surface Wave Devices," <u>J. Electrochem. Soc.,</u> Vol. 118, pp. 821-825 (May 1971).

3. D.L. Spears, and H.I. Smith, "High Resolution Pattern Replication Using Soft X-rays," <u>Electronic Letters</u>, Vol. 8, No. 4, pp. 102-104 (February 1972).

4. T.W.O'Keefe, "Fabrication of Integrated Circuits Using the Electron Image Projection Systems (ELIPS), " <u>IEEE Trans. Electron Devices,</u> Vol. ED-17, No. 6, pp. 465-469 (June 1970).

5. D.L. Kendall, "On Etching Very Narrow Grooves in Silicon <u>Appl. Phys. Letters.</u> Vol. 26, No. 4, pp. 195-198 (15 February 1975).

6. E.A.J. Marcatili, "Dielectric Rectangular Waveguides and Direc-tional Couplers for Integrated Optics," <u>BSTJ</u>, Vol. 48, pp. 2071-2102 (September 1969).

7. M.K. Barnoski, "<u>Introduction to Integrated Optics</u>," (Plenum Press, New York, New York, 1974). Chapter 6.

8. H.F. Taylor "Power Loss at Direction Changes in Dielectric Waveguides," <u>Appl. Optics,</u> Vol. 13, p. 642 (March 1974).